AIAA SciTech Forum
6-10 January 2025, Orlando, FL
AIAA SCITECH 2025 Forum

10.2514/6.2025-0420

Efficient Nonlinear Dynamic Analysis of Aircraft Structural Components with Various Boundary Conditions using the Koiter-Newton Model Reduction

Kautuk Sinha[1]
German Aerospace Center, Institute of Aeroelasticity, Goettingen, 37073, Germany

Farbod Alijani[2]
Delft University of Technology, Faculty of Mechanical Engineering, Mekelweg 2, 2628 CD Delft, Netherlands

Wolf R. Krueger[3]
German Aerospace Center, Institute of Aeroelasticity, Goettingen, 37073, Germany

Roeland De Breuker[4]
Delft University of Technology, Faculty of Aerospace Engineering, Kluyverweg 1, 2629 HS Delft, Netherlands

The evolving designs and requirements of aircraft structural components has recently created an increased interest in application of nonlinear modelling techniques. While the finite element (FE) methods already incorporate the necessary mechanics to model nonlinear behavior in structures, a major drawback is the considerably higher computation cost in comparison to the linear counterparts. Reduced order modelling (ROM) techniques offer a solution to counter this limitation. The work presented here is focused on the Koiter-Newton (K-N) model reduction technique which is based on a cubically nonlinear mechanical model. The K-N method utilizes existing FE models as a starting point to generate equivalent ROM parameters and thus, can be applied to obtain ROMs for generic structures. The model validity is assessed by conducting nonlinear dynamic analyses of two models with different boundary conditions. Nonlinear frequency response analyses are conducted to demonstrate hardening effects in both the test cases. Comparisons to full FE analyses show significant reduction in computational times.

I. Introduction

Engineering structures under conducive operational conditions can potentially exhibit various forms of nonlinearities arising from large strains, large deflections and contact conditions. Traditionally used linear formulations inherently neglect the mechanics that are responsible for nonlinear behavior and thus, can significantly deviate from the true structural response. Inclusion of nonlinearities, where applicable, already in the early design stages is crucial for a

[1] Researcher, Loads Analysis and Design.
[2] Associate Professor, Mechanical Engineering.
[3] Head of Department, Loads Analysis and Design
[4] Associate Professor and Head of Department, Aerospace Structures and Materials, AIAA Associate Fellow

better understanding of the structural response. Nonlinear analysis methods in the finite element (FE) framework are well developed, however, the existing drawback is the high computational effort needed. This is due to the utilization of predictor-corrector models with incremental loading which often require multiple iterations to achieve a converged response. The computational costs are further exacerbated when the applied loading is time dependent. The purpose of utilizing reduced order models (ROMs) for nonlinear analyses is to alleviate the computational burden while also obtaining a comparably accurate response.

Different kinematics of the structure demands different considerations when constructing a nonlinear model. For example, in bounded thin plates and curved panels subjected to bending loads, in-plane stretching of the structure is the dominant causative factor of nonlinear behavior. In such structures, nonlinearities can be observed already at deflection amplitudes in the order of the plate thickness. This type of nonlinearity results in early onset of amplitude dependent modal frequencies which have been extensively investigated in the past using several analytical and numerical ROMs [1]. Formulations derived from FE models are of interest since they can be applied to models of varying complexity. A review of non-intrusive ROM methods focusses on techniques that are applicable using standard outputs obtained from FE tools [2]. One of the first non-intrusive methods, based on ROM parameters computation using enforced displacements, presented in Ref. [3] was later utilized in Ref. [4] in combination with continuation methods. The use of continuation methods further speeds up the computation of nonlinear frequency response [4]. Recent developments in the use of modal derivatives for reduction subspace enrichment indicates the effectiveness of using higher order terms in the basis [5,6]. It is highlighted in Ref. [6] that the utilization of quadratic mapping of generalized displacements results in more accuracy in comparison to a linearly mapped model. Invariant manifold-based approaches have also been recently extended to high dimensional structural models for constructing nonlinear frequency response curves [7].

Cantilevered structures are highly influenced by nonlinear curvatures and large rotations at the free end resulting in the foreshortening effect [8]. This adds to the challenge of building ROMs for wing-like structures, especially using linear eigenmode based formulations since these are computed with small angle approximation and therefore, cannot directly provide information about the large in-plane motion. Moreover, the eigenmode shapes also exhibit some variation as the structure deforms. Recent investigations on flexible wing structures have demonstrated how geometric nonlinearities influence their static and eigenmode characteristics [9, 10]. Variants of eigenmode based approaches such as the ones utilizing higher order mode derivative components [11] and modal rotation components [12] have been found to be successful in improving the analysis efficiency. In the context of highly flexible wings, ROMs can be especially important for analyzing large amplitude response to dynamic loads and investigating dynamic instabilities.

The Koiter-Newton (K-N) method was originally developed for investigation of post-buckling behavior in thin plates [13]. The method was subsequently adopted for nonlinear dynamic analyses of thin plates with various boundary conditions [14]. Investigations pertaining to cantilevers revealed that the ROM developed in undeformed state of the structure has a limited domain of validity. This becomes increasingly apparent at greater deflections. A procedure to update the ROM at fixed load steps has been discussed in Refs. [15,16] which is found to improve the region of validity, however, also reduces the efficiency due to the additional ROM reconstructions required. In the K-N method, a modified governing equation of motion is considered comprising higher order stiffness tensors. The ROM is derived on the premise that the equilibrium path on the displacement space can be approximated using a Taylor series expansion. Eigenmode shapes in the reduction subspace, without requirement of mode subspace enrichment, have been found to be sufficient for this formulation. The present work aims to demonstrate the effectiveness of the K-N method in modelling the nonlinear dynamic response of different types of structures. Two verification cases are considered: (1) amplitude dependent frequency response of a rectangular plate structure constrained on parallel edges so that it exhibits a stretching based nonlinearity and, (2) nonlinear dynamic response of a highly flexible wing structure which is clamped on one end and undergoes large deflection motion. Comparisons are done against the full FE solutions from MSC Nastran in terms of the solution accuracy and computational time. The theoretical formulation of the K-N method and the results are discussed in the subsequent sections.

The remainder of the article is organized as follows: section II presents the theory behind the K-N model reduction, section III presents the structural models of the two test cases, in section IV the analysis results and comparisons to reference models are discussed and finally in section V the conclusions of the study are presented.

II. Koiter-Newton Model Reduction

The numerical formulation of the K-N method is presented in this section. For a detailed derivation of the ROM, the reader is referred to Refs. [13,14]. In its original form the approach is derived for a statics problem. The adaptations for nonlinear dynamics are subsequently discussed. The equations described in this section form the foundation of the K-N method.

The internal forces in a structure, as a function of the displacements $\boldsymbol{u}$, are described as $f_{int} = f(\boldsymbol{u})$. This can be expanded in the Taylor series in the form:

$$f(\boldsymbol{u}) = \boldsymbol{L}\boldsymbol{u} + \boldsymbol{Q}\boldsymbol{u}\boldsymbol{u} + \boldsymbol{C}\boldsymbol{u}\boldsymbol{u}\boldsymbol{u} + O(\|\boldsymbol{u}\|^4) \tag{1}$$

where ***L, Q, C*** are the linear, quadratic and cubic stiffness tensors, respectively. It is assumed that a linear subspace of the external force exists and can be parametrized by coordinates $\boldsymbol{\phi}$ along the predefined force vectors. The force subspace can be then described as:

$$\boldsymbol{f} = \boldsymbol{F}\boldsymbol{\phi} \tag{2}$$

where $\boldsymbol{F}$ consists of the external force vector, with *m* additional perturbation load vectors, if applicable, to model post buckling behavior. The equilibrium solution of Eq. (1) can be parametrized in terms of generalized displacements $\boldsymbol{\xi}$.

$$\boldsymbol{u} = \boldsymbol{u}_\alpha\boldsymbol{\xi} + \boldsymbol{u}_{\alpha\beta}\boldsymbol{\xi}\boldsymbol{\xi} + \boldsymbol{u}_{\alpha\beta\gamma}\boldsymbol{\xi}\boldsymbol{\xi}\boldsymbol{\xi} + O(\|\boldsymbol{\xi}\|^4) \tag{3}$$

where α, β, γ vary from 1,2…, *m*+1 and $\boldsymbol{u}_\alpha, \boldsymbol{u}_{\alpha\beta}, \boldsymbol{u}_{\alpha\beta\gamma}$ are the first, second and third order displacement fields respectively. These do not need to be presumed but rather are computed as by-products of the ROM parameter computation, as would be seen later. The parameterization in Eq. (3) can be fixed by choosing $\boldsymbol{\xi}$ such that it is a work conjugate to the load amplitudes $\boldsymbol{\phi}$, resulting in the equation:

$$(\boldsymbol{F}\boldsymbol{\phi})'\,\delta\boldsymbol{u} = \boldsymbol{\phi}'\delta\boldsymbol{\xi} \tag{4}$$

where the superscript prime indicates transpose. The load amplitude $\boldsymbol{\phi}$ is expanded consistent with the displacement expansion as:

$$\boldsymbol{\phi} = \bar{\boldsymbol{L}}\boldsymbol{\xi} + \bar{\boldsymbol{Q}}\boldsymbol{\xi}\boldsymbol{\xi} + \bar{\boldsymbol{C}}\boldsymbol{\xi}\boldsymbol{\xi}\boldsymbol{\xi} + O(\|\boldsymbol{\xi}\|^4) \tag{5}$$

Equations (3) and (5) are substituted into Eq. 1 which is solved for the coefficients of the $\boldsymbol{\xi}$ terms. Additionally, Eq. (3) is substituted into Eq. (4) to obtain orthogonality constraint equations. Together these form the set of equations required for obtaining the ROM parameters $\bar{\boldsymbol{L}}, \bar{\boldsymbol{Q}}, \bar{\boldsymbol{C}}$ and the displacement fields required for reconstructing the actual displacements from the generalized displacements.

$$\begin{bmatrix} \boldsymbol{L} & -\boldsymbol{F} \\ -\boldsymbol{F}' & \boldsymbol{0} \end{bmatrix} \begin{Bmatrix} \boldsymbol{u}_\alpha \\ \bar{\boldsymbol{L}}_\alpha \end{Bmatrix} = \begin{Bmatrix} \boldsymbol{0} \\ -\boldsymbol{E}_\alpha \end{Bmatrix} \tag{6}$$

$$\begin{bmatrix} \boldsymbol{L} & -\boldsymbol{F} \\ -\boldsymbol{F}' & \boldsymbol{0} \end{bmatrix} \begin{Bmatrix} \boldsymbol{u}_{\alpha\beta} \\ \bar{\boldsymbol{Q}}_{\alpha\beta} \end{Bmatrix} = \begin{Bmatrix} -\boldsymbol{Q}(\boldsymbol{u}_\alpha, \boldsymbol{u}_\beta) \\ \boldsymbol{0} \end{Bmatrix} \tag{7}$$

$$\bar{\boldsymbol{C}}_{\alpha\beta\gamma\delta} = \boldsymbol{C}(\boldsymbol{u}_\alpha, \boldsymbol{u}_\beta, \boldsymbol{u}_\gamma, \boldsymbol{u}_\delta) - \frac{2}{3}\left[\boldsymbol{u}'_{\alpha\beta}\,\boldsymbol{L}\,\boldsymbol{u}_{\delta\gamma} + \boldsymbol{u}'_{\beta\gamma}\,\boldsymbol{L}\,\boldsymbol{u}_{\delta\alpha} + \boldsymbol{u}'_{\gamma\alpha}\,\boldsymbol{L}\,\boldsymbol{u}_{\delta\beta}\right] \tag{8}$$

In Eq. (6), $\boldsymbol{E}_\alpha$ is a vector whose α^{th} entry is one and all other terms are zero. For application to the nonlinear dynamics, momentum subspace is utilized in the reduction basis instead of the external force vector. It has been shown in Ref. [14] that the utilization of momentum subspace results in a system of equations analogous to Eqs. (6)-(8). The use of the momentum subspace also enables us to easily compute mass and damping matrices in the ROM subspace.

Similar to Eq. (2), it is assumed that the momentum $\boldsymbol{p}$ is parameterized by coordinates $\boldsymbol{\pi}$, as:

$$\boldsymbol{p} = \boldsymbol{P}\boldsymbol{\pi} \tag{9}$$

where $\boldsymbol{P}$ is the basis matrix for the model reduction and comprises the product of the mass matrix and a modal matrix $\boldsymbol{\varphi}$ with selected eigenmodes. The number of eigenmodes selected in the basis matrix determines the size of the ROM. It is also important to note that inclusion of only bending modes is insufficient to capture the twist response. At least one torsion mode must be selected in the basis matrix when torsion loads are acting on the structure. With this adaptation of the momentum subspace, $\boldsymbol{P}$ replaces the load matrix $\boldsymbol{F}$ in the Eq. (6)-(7). All other parameters remain same in the Eqs. (6)-(8).

By considering the total kinetic energy of the system, the reduced mass matrix $\bar{\boldsymbol{M}}$ can be then identified as:

$$\bar{\boldsymbol{M}} = (\boldsymbol{\varphi}'\boldsymbol{M}\,\boldsymbol{\varphi})^{-1} \tag{10}$$

where $\boldsymbol{\varphi}'$ indicates the transpose of the modal matrix.

The reduced damping matrix is identified by considering a quadratic damping model and given as:

$$\bar{\boldsymbol{D}} = \bar{\boldsymbol{M}}\,(\boldsymbol{P}'\boldsymbol{M}^{-1}\boldsymbol{D}\,\boldsymbol{M}^{-1}\,\boldsymbol{P})\,\bar{\boldsymbol{M}} \tag{11}$$

where $\boldsymbol{M}$ is the mass matrix and $\boldsymbol{D}$ is the damping matrix in the full FE model.

The equation of motion for nonlinear dynamics in the ROM subspace can be then expressed as:

$$\bar{\boldsymbol{M}}\,\ddot{\boldsymbol{\xi}} + \bar{\boldsymbol{D}}\,\dot{\boldsymbol{\xi}} + \bar{\boldsymbol{L}}\,\boldsymbol{\xi} + \bar{\boldsymbol{Q}}\,\boldsymbol{\xi}\boldsymbol{\xi} + \bar{\boldsymbol{C}}\,\boldsymbol{\xi}\boldsymbol{\xi}\boldsymbol{\xi} = \boldsymbol{\phi}(t) \tag{12}$$

The reduced force component $\boldsymbol{\phi}$ of the Eq. (12) is computed as $\boldsymbol{u}'_{\alpha}\boldsymbol{f}$.

The time domain solution of the generalized displacements is obtained by solving Eq. (12) using the Newmark time integration scheme. The solution is then substituted in Eq. (3) in order to compute the real structural displacements for each time step. The computation of nonlinear frequency response curves is done with the aid of parametric continuation method in the software AUTO [17]. ROM parameters are normalized for the AUTO analyses in order to ensure numerical stability. The procedure for the normalization is described in Ref. [14]. The continuation approach is significantly faster than using a brute force strategy of computing the time domain response at several frequency steps and extracting the peak displacement amplitudes in each step.

The main inputs required to obtain the ROM parameters are the stiffness tensors, mass matrix, damping matrix and the external force vector from a full FE model. Additionally, the selected eigenmode shapes obtained from a linear eigenvalue analysis are required to construct the ROM basis. Most of these are obtainable directly from standard FE solvers. To obtain the higher order stiffness tensors (quadratic and cubic) a strain energy-based approach is utilized. In this method, the strain energy for each element is derived in variable form and the higher order analytical derivatives of the strain energy provide the quadratic and cubic stiffness terms of each element [13,14]. This is then subjected to a global assembly process in order to obtain the higher order stiffness tensors. The analysis framework used here is built upon the usage of a high-performance triangular shell element [18]. The relevant element formulations are listed in the Appendix.

III. Structural Models

Two test cases are considered in this work: (1) Beam with both ends clamped, (2) the highly flexible benchmark Pazy wing. The general characteristics of the structural models are described in this section.

A. Clamped-clamped beam

The model is chosen from Ref. [19] where nonlinear frequency response has been constructed using a non-intrusive eigenmode based ROM. The beam dimensions are specified as following: length l = 1 m, width b = 0.05 m, and

thickness t = 1 mm. The material properties of the beam are: elastic modulus E = 210 GPa, density ρ = 7800 kg/m^3 and Poisson's ratio $\nu = 0$. Similar to the reference work, the structure is modelled as a slender rectangular plate using shell elements. The mesh generated results in 707 FE nodes and 4242 degrees of freedom (DOFs). The beam is fully clamped i.e. all 6 DOFs are constrained, on two of its parallel shorter edges measuring 0.05 m. Such boundary conditions or its variants are often used as an approximation when analyzing local deformation behavior in sub-structural components. An initial model check is performed by comparing the linear eigenfrequencies to the data presented in Ref. [19] where the mesh is generated using rectangular shell elements and consists of 505 FE nodes. The comparison is presented in Table 1.

Table 1 Comparison of linear eigenfrequencies of the clamped-clamped beam

Mode number	Reference [Hz]	Current [Hz]
1	5.33	5.22
2	14.70	14.38
3	28.82	28.21
4	47.64	46.64
5	71.17	69.69

B. Pazy wing benchmark model

The Pazy wing is an experimental benchmark model designed and developed at Technion for tip deflections up to 50% of the span [20]. The model utilized in this work is based on the design parameters of the Pazy wing. To be able to import it into our analysis framework, the model has been constructed entirely using shell elements and due to this, adaptations were made which resulted in minor differences from the original design. The wing spans across 0.56 m and has a chord length of 0.11 m. The cross-section profiles are modelled using the standard NACA0018 airfoil.

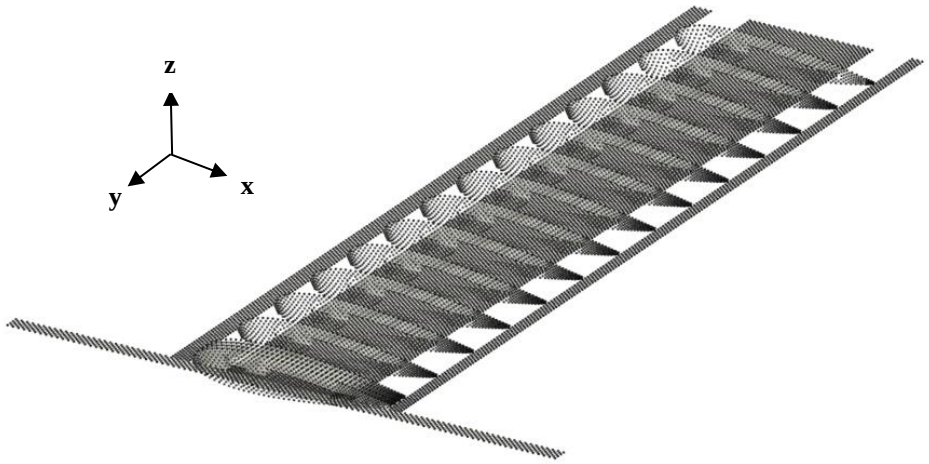

Fig. 1 Pazy wing finite element model

The central rectangular plate is made of Aluminum 7075 and the surrounding frame structure (including the ribs and the beam structures at the leading edge, trailing edge and the wing tip, as shown in Fig. 1) are made of Nylon 12. The mesh generated in the FE model results in 39,930 triangular shell elements and 21,712 nodes. The model is fully clamped at the root i.e. all 6 DOFs of all the nodes at the wing root are constrained. In prior studies of the Pazy wing, the difficulties in modelling the skin is highlighted, which undergoes buckling at low load levels [21]. Therefore, the skin is excluded in the current model. For validating the mass and stiffness matrix formulations, the first five linear eigenfrequencies of the model are compared in Table 2 to the reference FE model, which is relatively coarsely meshed

with 8134 FE nodes, and the eigenfrequencies of the current model computed in MSC Nastran. The nonlinear static behavior has been previously compared against Nastran results in Ref. [22] which provides a good validation for the nonlinear stiffness formulation.

Table 2 Comparison of linear eigenfrequencies of the Pazy wing

Mode number	Mode shape	Reference model Nastran [Hz]	Current model Nastran [Hz]	Current model Matlab [Hz]
1	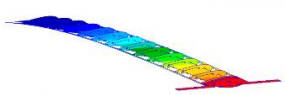	4.42	4.28	4.28
2	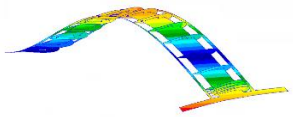	28.98	28.12	28.15
3	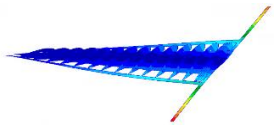	40.33	38.49	39.47
4	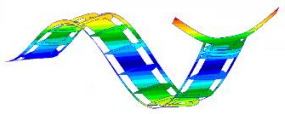	82.40	80.17	80.39
5	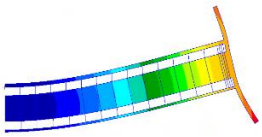	112.56	111.5	111.75

IV. Results

A. Nonlinear frequency response of the beam

Beam structures which are constrained on both ends tend to exhibit a high degree of non-linearity when deflected to amplitudes in the order of their cross-sectional thickness. The beam structure considered here has been studied in Ref. [19] where the forced vibration response at different amplitudes and the backbone curves corresponding to the nonlinear normal modes are presented. The authors utilize a non-intrusive reduced order modelling approach where a combination of transverse and axial mode shapes is used in the modal basis. In total 10 transverse bending modes and 31 axial modes were used for computing the ROM parameters in Ref. [19]. The same analysis is conducted in this study for the first eigenfrequency using the K-N method. The analysis parameters are chosen in accordance with the

description in Ref. [19]. With the origin of the structural coordinate system considered on a fixed edge, the beam structure is excited at a location x = 0.32 m, y = 0.025 m and the damping ratio is fixed at 2 %. A forced nonlinear frequency response is constructed by doing a frequency sweep in the proximity of the first linear eigenfrequency. The maximum amplitude at the excitation point for each frequency step is extracted. As discussed in section II, the frequency sweep is done using the parametric continuation in AUTO. Nonlinear frequency response curves are constructed for six load amplitudes: 0.001 N, 0.004 N, 0.008 N, 0.011 N, 0.014 N and 0.017 N. The highest load amplitude is such that the peak vibration amplitudes surpass the cross-sectional thickness. These forced frequency response curves are superimposed with the backbone curve presented in Ref. [19] for comparison. The vibration amplitude is normalized by the thickness and the applied excitation frequency is normalized by the first linear eigenfrequency.

In Fig. 2a it is shown that the reference backbone curve approximately passes through the peaks of each of the forced nonlinear frequency response curve which is in accordance with the expected behavior. The structure exhibits a hardening type nonlinearity which implies that the eigenfrequency increases as the amplitude of vibration increases, in this case, increasing by almost 40 %. The ROM parameters in the K-N method are computed using the first five linear eigenmodes in the basis matrix which results in a 5-DOF model. Since the K-N method inherently incorporates the coupling of in-plane and transverse motion in the higher order displacement fields, there is no necessity of computing and explicitly searching for axial modes to account for in-plane motion. The pre-processing for this model, including the formulation of stiffness and mass matrices, eigenvalue analysis and computation of the ROM parameters, requires 11.2 s. The ROM parameters are provided as an input to AUTO for parametric continuation which requires approximately 48 s for computing the frequency response curve at the maximum load.

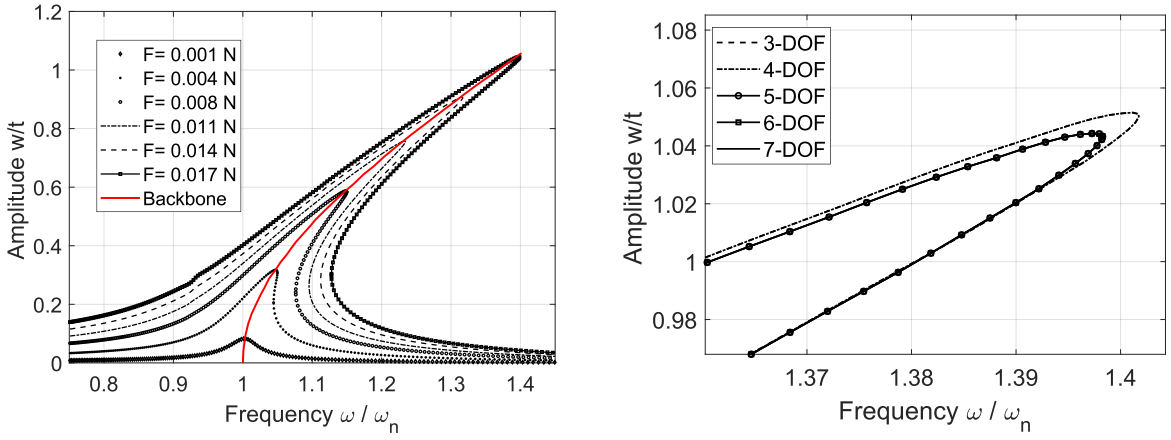

(a) Comparison to the backbone curve (b) Magnified view at the peak amplitude

Fig. 2 Nonlinear frequency response curves of the first mode of the beam

A convergence study is conducted to assess the influence of adding eigenmodes to the ROM basis. Figure 2b shows a magnified view of the comparison of the frequency response curves at the maximum applied force generated with different number of modes in the ROM basis. In the figure, *N*-DOF refers to the first *N* linear eigenmodes considered in the ROM basis. The use of 3- and 4-DOF models results in a slightly stiffer response with a difference in amplitude of ~0.5 % at the normalized frequency of 1.397. The 5-, 6- and 7-DOF models produce precisely the same response which also matches with the expected trend based on the backbone curve. A 5-DOF ROM is therefore sufficient to model the frequency variation at the shown amplitudes.

B. Nonlinear dynamic response of the Pazy wing

The Pazy wing FE model consists of a relatively larger number of nodes which adds to the challenge of conducting a numerically efficient nonlinear analysis. In this work we study the steady state response of the wing under continuous harmonic excitation. A tip load is added at the mid-chord position which is a sine function of time at an excitation

frequency equal to the first eigenfrequency. The analysis is first conducted using MSC Nastran with an applied load of 2.2 N. Due to difficulty in obtaining a converged response in Nastran, a higher damping ratio of 0.13 is utilized. The chosen analysis parameters result in a moderately large tip deflection of around 20 % of the span. The analysis is conducted with adaptive time step increments with an initial time increment of 0.0005 s and reaches completion in 12.8 hours. In the K-N method, the ROM is constructed by sequentially using the first few eigenmodes in the ROM basis. Variants of the model with 1- to 5-DOFs are considered and it is seen that there are negligible differences in the corresponding solutions i.e. a 1-DOF ROM computes a sufficiently accurate response. Figure 3 depicts a comparison between the Nastran solution and the ROM solutions obtained using 1- and 5-DOF models. The solution obtained from the K-N method differs by 1.6 % in the transverse direction and 1.7 % in the spanwise in-plane direction. The analysis using the 1-DOF model requires 6.5 s and the analysis using the 5-DOF model requires 27 s. The preprocessing for computation of ROM parameters required 11.9 mins for the 1-DOF model and around 3 hours for the 5-DOF model. Thus, bulk of the computation time in the K-N method goes into the formulation of the ROM parameters and this becomes especially prominent for large FE models.

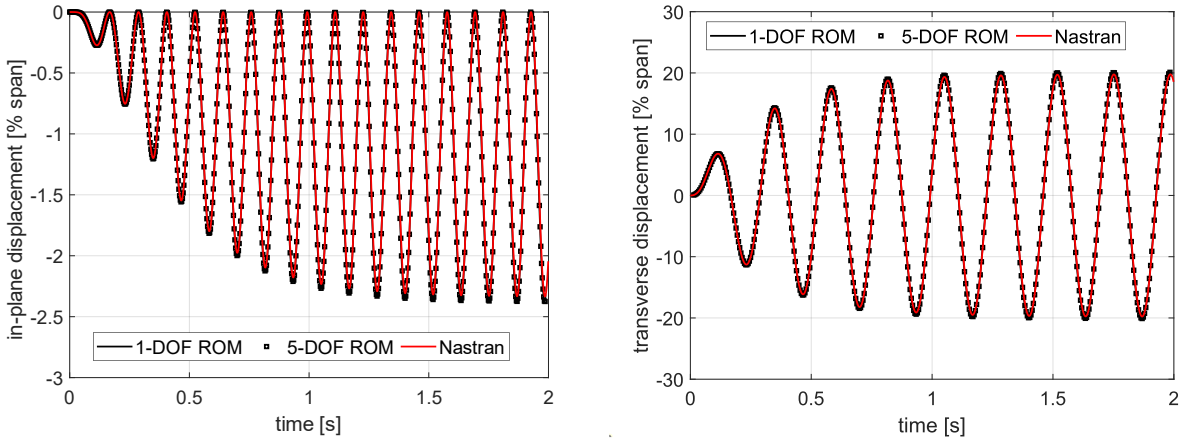

(a) In-plane displacement in spanwise direction (b) Transverse displacement

Fig. 3 Steady state response of the Pazy wing at 2.2 N tip force, 0.13 damping

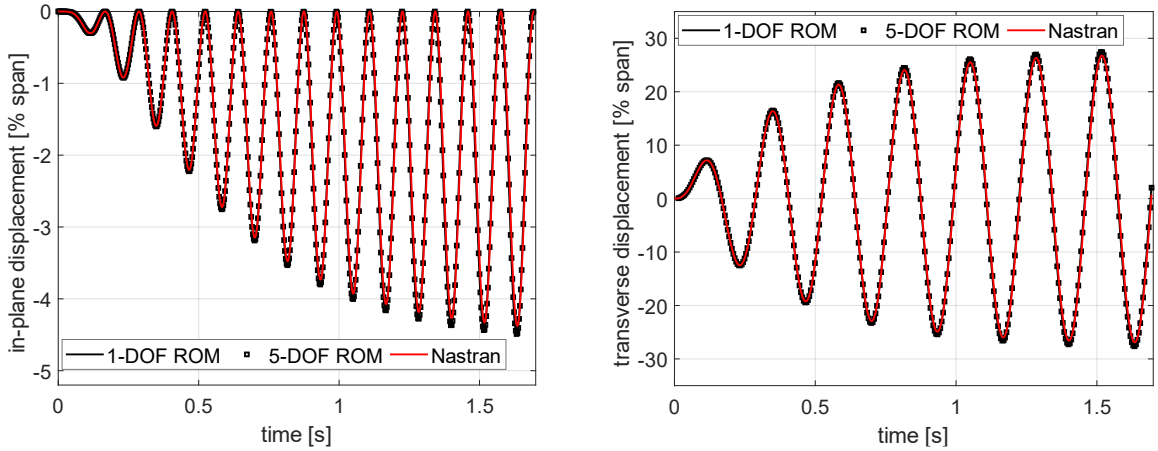

(a) In-plane displacement in spanwise direction (b) Transverse displacement

Fig. 4 Steady state response of the Pazy wing at 2.2 N tip force, 0.093 damping

If the damping ratio is reduced to 0.093, it results in transverse displacements up to 27 % of the span. However, at these increased amplitudes the Nastran solver does not converge at time step t = 1.694 s. The K-N model does not face convergence problems due to the highly reduced model size. Comparison of the transverse displacements and in-plane displacement for this case in spanwise direction is shown in Fig. 4. If comparisons are made at the last converged peak in the response, the K-N model differs by 2.5 % in the spanwise in-plane direction and 2.6 % in the transverse direction.

The modal characteristics of the Pazy wing has been investigated in earlier works [9, 21, 22] where it has been shown that the eigenfrequencies tend to change as the wing undergoes large deflections. This variation is captured by computing the wing deflections with inclusion of geometric nonlinearities and subsequently, computing the eigenfrequencies in the deformed state of the wing. Using this approach, strong variations are seen especially in the first torsion and in-plane modes while the first three bending modes show marginal variations. In this work, we investigate the amplitude-frequency dependency in the nonlinear normal mode sense i.e. the behavior of the eigenfrequencies in the case of large amplitude vibrations. A frequency sweep is conducted in the neighborhood of the frequencies of interest and the peak amplitude for each frequency step is extracted. The first transverse (Mode 1) and lateral bending (Mode 5) modes are considered for these analyses. The proportional damping coefficient is fixed such that damping ratio of the transverse bending mode is 0.093 and of the lateral bending mode is 0.0036. The time domain analyses conducted established that 1-DOF model can be utilized with reasonable response accuracy. Different ROM bases are chosen for the two modes - the eigenvector corresponding to the Mode 1 for the transverse bending case and the eigenvector corresponding to the Mode 5 for the lateral bending case. Three force amplitudes – 0.1 N, 0.2 N, 0.3 N, are applied in steps and the nonlinear frequency response is obtained for each load case in transverse bending. Similarly, for the lateral bending case, we consider the load amplitudes 20 N, 30 N and 40 N. The frequency response curves of the Pazy wing are depicted in Fig. 5 where the applied frequency step is normalized by the eigenfrequency and the resultant response amplitude is normalized by the span. The amplitudes considered in the Figs. 5a and 5b are transverse and in-plane displacements, respectively.

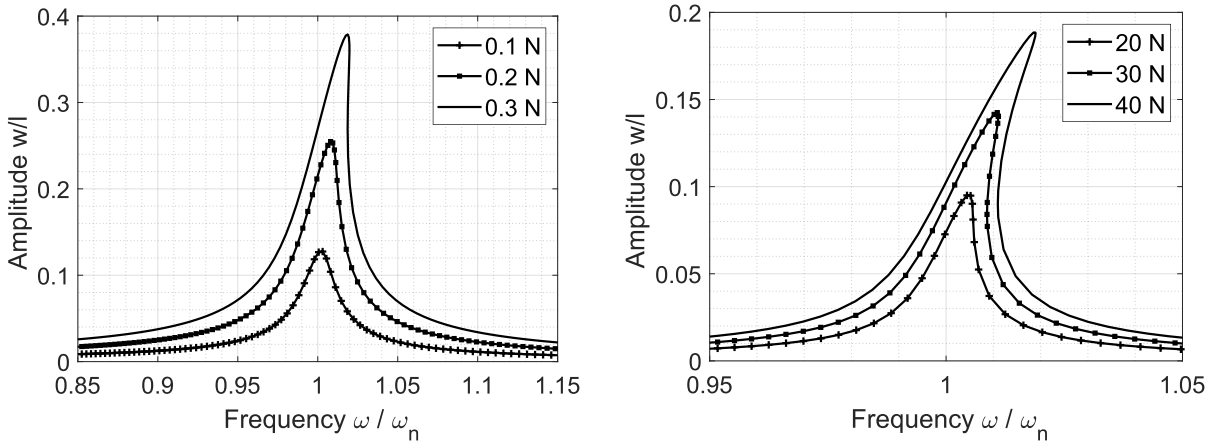

(a) Transverse bending mode

(b) Lateral bending mode

Fig. 5 Nonlinear frequency response curves of the Pazy wing

The transverse bending mode shows only a slight shift of 1.9 % in the frequency peak at an amplitude of ~ 38 % of the span. In comparison, the lateral bending mode shows a relatively early onset of the frequency variation and changes by 1.9 % when the response amplitude is around 19 % of the span. Such dynamic response amplitudes are generally beyond normal operational conditions of aircraft structures. However, it is notable that these analyses have been conducted for the undeformed wing. It may be of greater interest to compute such nonlinear frequency response curves of a wing subjected to a prior static deflection. Since a 1-DOF model is utilized for these analyses, the simulation times are greatly reduced and is less than 2 mins for each load case. All simulations were executed on a Linux system with an Intel(R) Xeon(R) W-2145 CPU @ 3.70GHz processor and 32Gb RAM.

V. Conclusions

The K-N method is utilized to perform nonlinear analyses on two test cases with different boundary conditions and comparisons were made with results from earlier publications and with Nastran computations. Results pertaining to time domain simulations as well as nonlinear frequency response curves have been presented. The first test case, representative of various sub-structural components, is utilized to demonstrate hardening effects in clamped-clamped structures at vibration amplitudes in the order of structural thickness. The K-N method is closely able to replicate the reference backbone curve while utilizing a reduced 5-DOF model. A frequency shift of almost 40 % is seen when the vibration amplitudes are similar to the thickness of the beam. The second test case with increased model complexity is utilized to demonstrate the significantly reduced computational time achievable. For the Pazy wing, the K-N method reduces the computational time by up to 98 % in time domain analyses with harmonic excitations while limiting the solution error to less than 3 %. Finally, nonlinear frequency response curves are presented for the Pazy wing. In this case, the observable frequency shifts only occur at amplitudes greater than 20 % of the span. A 1-DOF model is utilized in these analyses, therefore, the simulation times are significantly reduced to less than 2 min per load case.

Appendix

Higher order stiffness terms are derived from the strain energy formulations. Triangular shell elements developed in [18] are utilized. Detailed expressions can be found in [23].

Total strain in a deformed state $\boldsymbol{q}$ is defined as:

$$\varepsilon = \varepsilon_l + \varepsilon_{nl} = (\boldsymbol{B_l} + \frac{1}{2}\boldsymbol{B_{nl}}(\boldsymbol{q}))\boldsymbol{q}$$

$$\boldsymbol{B_l} = \frac{1}{2A}[\boldsymbol{B_1}\,\boldsymbol{B_2}\,\boldsymbol{B_3}],$$

where *A* is the element area.

Considering that the three nodal coordinates are *(x1, y1), (x2, y2)* and *(x3, y3),*

$$x_{ij} = x_i - x_j$$
$$x_{ij} = x_i - x_j$$

$$\boldsymbol{B_1} = \begin{bmatrix} y_{23} & 0 & 0 & 0 & 0 & \frac{y_{23}(y_{13}-y_{21})}{6} \\ 0 & x_{23} & 0 & 0 & 0 & \frac{x_{32}(x_{32}-x_{12})}{6} \\ x_{32} & y_{32} & 0 & 0 & 0 & \frac{x_{31}y_{13}-x_{12}y_{21}}{3} \end{bmatrix}$$

$$\boldsymbol{B_2} = \begin{bmatrix} y_{31} & 0 & 0 & 0 & 0 & \frac{y_{31}(y_{21}-y_{32})}{6} \\ 0 & x_{13} & 0 & 0 & 0 & \frac{x_{13}(x_{12}-x_{23})}{6} \\ x_{13} & y_{31} & 0 & 0 & 0 & \frac{x_{12}y_{21}-x_{23}y_{32}}{3} \end{bmatrix}$$

$$\boldsymbol{B_2} = \begin{bmatrix} y_{12} & 0 & 0 & 0 & 0 & \frac{y_{12}(y_{32}-y_{13})}{6} \\ 0 & x_{21} & 0 & 0 & 0 & \frac{x_{21}(x_{23}-x_{31})}{6} \\ x_{21} & y_{12} & 0 & 0 & 0 & \frac{x_{23}y_{32}-x_{31}y_{13}}{3} \end{bmatrix}$$

The nonlinear strain component can be computed using the $\boldsymbol{B_{nl}}(\boldsymbol{q})$ term which is given by:

$$\boldsymbol{B}_{nl}(\boldsymbol{q}) = \begin{bmatrix} \boldsymbol{q}^t\, K_{xx} \\ \boldsymbol{q}^t\, K_{yy} \\ \boldsymbol{q}^t\, K_{xy} \end{bmatrix}$$

$$\boldsymbol{K_{xx}} = \boldsymbol{B}_w^t \boldsymbol{T}_x^t \boldsymbol{T}_x \boldsymbol{B}_w + \boldsymbol{B}_v^t \boldsymbol{T}_x^t \boldsymbol{T}_x \boldsymbol{B}_v$$

$$\boldsymbol{K_{yy}} = \boldsymbol{B}_w^t \boldsymbol{T}_y^t \boldsymbol{T}_y \boldsymbol{B}_w + \boldsymbol{B}_u^t \boldsymbol{T}_y^t \boldsymbol{T}_y \boldsymbol{B}_u$$

$$\boldsymbol{K_{xy}} = \boldsymbol{B}_w^t (\boldsymbol{T}_x^t \boldsymbol{T}_y + \boldsymbol{T}_y^t \boldsymbol{T}_x) \boldsymbol{B}_w$$

Here,

$$\boldsymbol{T}_x = \frac{1}{2A} [\, y_{23}\; y_{31}\; y_{12}] \text{ and } \boldsymbol{T}_y = \frac{1}{2A} [\, x_{32}\; y_{13}\; x_{21}]$$

The other symbols $\boldsymbol{B}_u$, $\boldsymbol{B}_v$, $\boldsymbol{B}_w$ represent 3 x 18 matrices. In $\boldsymbol{B}_u$ the terms at (1,1), (2,7), and (3,13) are 1 and all other terms are zero. In $\boldsymbol{B}_v$ the terms at (1,2), (2,8), and (3,14) are 1 and all other terms are zero. Similarly, in $\boldsymbol{B}_w$ the terms at (1,3), (2,9), and (3,15) are 1 and all other terms are zero.

The internal force **f**, tangent stiffness **L,** quadratic stiffness **Q** and cubic stiffness **C** are derived as derivatives of the strain energy with respect to the displacement.

$$\boldsymbol{f} = A(\boldsymbol{B}_l{}' \boldsymbol{N}_{nl} + \boldsymbol{B}_{nl}{}' \boldsymbol{N})$$

$$\boldsymbol{L} = A\,(\boldsymbol{B}_l{}' \boldsymbol{A}_m \boldsymbol{B}_{nl} + \boldsymbol{B}_{nl}{}' \boldsymbol{A}_m \boldsymbol{B}_l + \boldsymbol{B}_{nl}{}' \boldsymbol{A}_m \boldsymbol{B}_{nl} + \boldsymbol{N}_x \boldsymbol{K_{xx}} + \boldsymbol{N}_y \boldsymbol{K_{yy}} + \boldsymbol{N_{xy}} \boldsymbol{K_{xy}})$$

$$\boldsymbol{N} = \boldsymbol{N_l} + \boldsymbol{N_{nl}} = \boldsymbol{A_m} \boldsymbol{B_l} \boldsymbol{q} + \frac{1}{2} \boldsymbol{A_m} \boldsymbol{B_{nl}}(\boldsymbol{q}) \boldsymbol{q}$$

$$\boldsymbol{Q}(\boldsymbol{u}_\alpha, \boldsymbol{u}_\beta) = \frac{A}{2} (\boldsymbol{B}'_{nl}(\boldsymbol{u}_\beta) \boldsymbol{A}_m \boldsymbol{B}(\boldsymbol{u}_\alpha) \boldsymbol{u}_\alpha + \boldsymbol{B}'_{nl}(\boldsymbol{u}_\alpha) \boldsymbol{A}_m \boldsymbol{B}(\boldsymbol{u}_\beta) \boldsymbol{u}_\beta + \boldsymbol{B}' \boldsymbol{A}_m \boldsymbol{B}_{nl}(\boldsymbol{u}_\alpha) \boldsymbol{u}_\beta)$$

$$\boldsymbol{C}(\boldsymbol{u}_\alpha, \boldsymbol{u}_\beta, \boldsymbol{u}_\gamma, \boldsymbol{u}_\delta) = \frac{A}{6} (\boldsymbol{A}_m \boldsymbol{B}_{nl}(\boldsymbol{u}_\alpha) \boldsymbol{u}_\delta \boldsymbol{B}_{nl}(\boldsymbol{u}_\beta) \boldsymbol{u}_\gamma + \boldsymbol{A}_m \boldsymbol{B}_{nl}(\boldsymbol{u}_\beta) \boldsymbol{u}_\delta \boldsymbol{B}_{nl}(\boldsymbol{u}_\alpha) \boldsymbol{u}_\gamma + \boldsymbol{A}_m \boldsymbol{B}_{nl}(\boldsymbol{u}_\gamma) \boldsymbol{u}_\delta \boldsymbol{B}_{nl}(\boldsymbol{u}_\alpha) \boldsymbol{u}_\beta)$$

References

[1] Alijani, F. and Amabili, M., "Non-linear vibrations of shells: A literature review from 2003 to 2013". *International journal of non-linear mechanics*, Vol. 58, pp. 233-257, 2014.

[2] Mignolet, M. P., Przekop, A., Rizzi, S. A., and Spottswood, S. M., "A review of indirect/non-intrusive reduced order modeling of nonlinear geometric structures", *Journal of Sound and Vibration*, Vol. 332(10), pp. 2437-2460, 2013.

[3] Muravyov, A.A. and Rizzi, S.A. "Determination of nonlinear stiffness with application to random vibration of geometrically nonlinear structures". *Computers & Structures*, Vol. 81(15), pp.1513-1523, 2003

[4] Kuether, R.J., Deaner, B.J., Hollkamp, J.J. and Allen, M.S., "Evaluation of geometrically nonlinear reduced-order models with nonlinear normal modes", *AIAA Journal*, Vol. 53(11), pp.3273-3285, 2015.

[5] Idelsohn, S.R. and Cardona, A., "A reduction method for nonlinear structural dynamic analysis", *Computer Methods in Applied Mechanics and Engineering*, Vol. 49(3), pp.253-279, 1985.

[6] Jain, S., Tiso, P., Rutzmoser, J.B. and Rixen, D.J., "A quadratic manifold for model order reduction of nonlinear structural dynamics", *Computers & Structures*, Vol. 188, pp.80-94, 2017.

[7] Jain, S. and Haller, G., "How to compute invariant manifolds and their reduced dynamics in high-dimensional finite element models". *Nonlinear dynamics*, Vol. 107(2), pp.1417-1450, 2022.

[8] Bisshopp, K.E. and Drucker, D.C., "Large deflection of cantilever beams". *Quarterly of applied mathematics*, Vol. 3(3), pp.272-275, 1945.

[9] Riso, C. and Cesnik, C.E., "Geometrically nonlinear effects in wing aeroelastic dynamics at large deflections", *Journal of Fluids and Structures*, Vol. 120, p.103897, 2023.

[10] Drachinsky, A. and Raveh, D.E., "Nonlinear aeroelastic analysis of highly flexible wings using the modal rotation method", *AIAA Journal*, Vol. 60(5), pp.3122-3134, 2022.

[11] Ritter, M.R., "An extended modal approach for nonlinear aeroelastic simulations of highly flexible aircraft structures", Ph.D. Dissertation, Technische Universitaet Berlin (Germany), 2019.

[12] Drachinsky, A. and Raveh, D.E., "Modal rotations: A modal-based method for large structural deformations of slender bodies", *AIAA Journal*, 58(7), pp.3159-3173, 2020.

[13] Liang, K., Abdalla, M. and Gürdal, Z., "A Koiter-Newton approach for nonlinear structural analysis", *International Journal for Numerical Methods in Engineering*, Vol. 96(12), pp.763-786, 2013.

[14] Sinha, K., Singh, N.K., Abdalla, M.M., De Breuker, R. and Alijani, F., "A momentum subspace method for the model-order reduction in nonlinear structural dynamics: Theory and experiments", *International Journal of Non-Linear Mechanics*, Vol. 119, p.103314, 2020.

[15] Sinha, K., Alijani, F., Krüger, W.R. and De Breuker, R., 2023. Koiter–Newton Based Model Reduction for Large Deflection Analysis of Wing Structures. AIAA Journal, Vol. 61(8), pp.3608-3617, 2023.

[16] Sinha, K., Alijani, F., Krüger, W.R. and De Breuker, R., "Nonlinear dynamics of wing-like structures using a momentum subspace-based Koiter-Newton reduction", *Journal of Sound and Vibration*, Vol. 596, p.118747, 2025.

[17] Doedel, E.J., "AUTO: A program for the automatic bifurcation analysis of autonomous systems", *Congr. Numer*, Vol. 30(265-284), pp.25-93, 1981.

[18] Militello, C. and Felippa, C.A., "The first ANDES elements: 9-dof plate bending triangles", *Computer methods in applied mechanics and engineering*, Vol. 93(2), pp.217-246, 1991.

[19] Givois, A., Grolet, A., Thomas, O. and Deü, J.F., "On the frequency response computation of geometrically nonlinear flat structures using reduced-order finite element models", *Nonlinear Dynamics*, Vol. 97(2), pp.1747-1781, 2019.

[20] Avin, O., Raveh, D.E., Drachinsky, A., Ben-Shmuel, Y. and Tur, M., "An experimental benchmark of a very flexible wing", *In AIAA Scitech 2021 Forum*, (p. 1709), 2021.

[21] Ritter, M., Hilger, J. and Zimmer, M., "Static and dynamic simulations of the Pazy wing aeroelastic benchmark by nonlinear potential aerodynamics and detailed FE model", In *AIAA Scitech 2021 forum*, p. 1713, 2021.

[22] Sinha, K., Alijani, F., Krueger, W.R. and De Breuker, R., "Nonlinear dynamic response of a Pazy wing variant using Koiter-Newton model reduction", In *International Forum on Aeroelasticity and Structural Dynamics*, 2024.

[23] Liang, K., "A Koiter-Newton arclength method for buckling-sensitive structures", Ph.D. Dissertation, Delft University of Technology, 2013